Supplementary Material

Room-temperature discrete-charge-fluctuation dynamics of a single molecule adsorbed on a carbon nanotube

Agung Setiadi[a], Hayato Fujii[a], Megumi Akai-Kasaya[a]*, Seiya Kasai[b], Ken-ichi Yamashita[c], Takuji Ogawa[c], Takashi Ikuta[d], Yasushi Kanai[d], Kazuhiko Matsumoto[d], Yuji Kuwahara[a]

[a]*Department of Precision Science and Technology, Graduate School of Engineering, Osaka University, 565-0871 Suita, Japan. Email: kasaya@prec.eng.osaka-u.ac.jp*
[b]*Research Center for Integrated Quantum Electronics, Hokkaido University, 060-8628 Sapporo, Japan.*
[c]*Department of Chemistry, Graduate School of Science, Osaka University, 560-0043 Toyonaka, Japan.*
[d]*The Institute of Scientific and Industrial Research, Osaka University, 567-0047 Ibaraki, Japan.*

Atomic force microscope images before and after adsorption of PMo_{12}

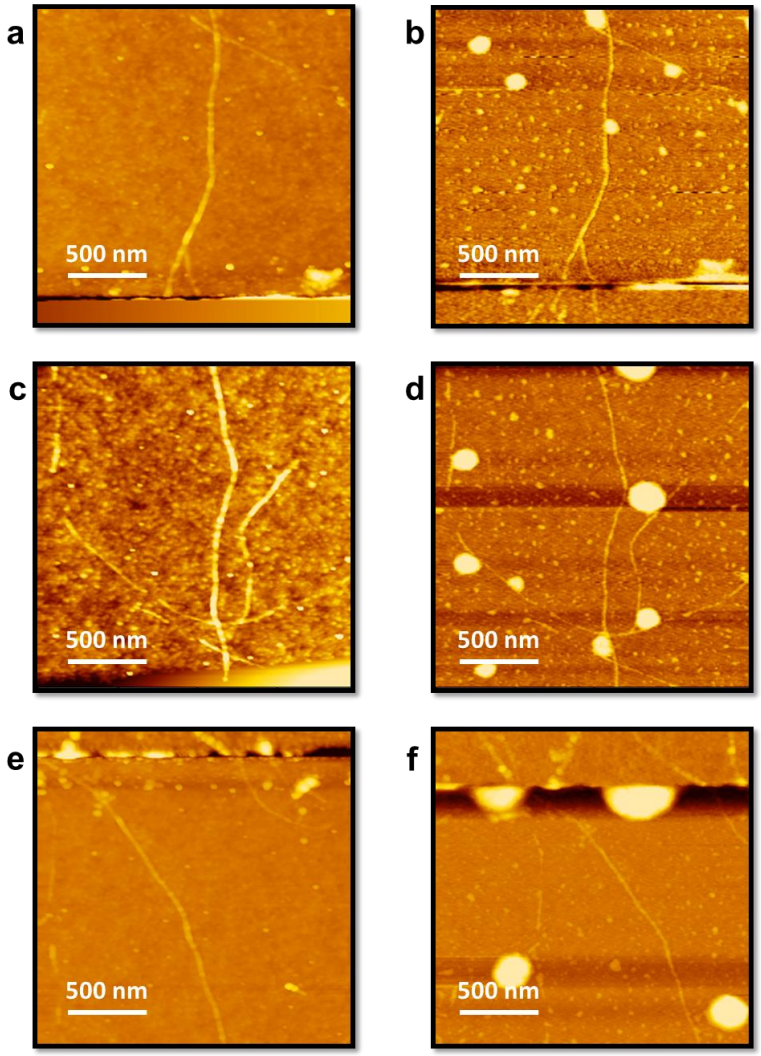

Figure S1. AFM images of the CNT device before ((a), (c), and (e)) and after ((b), (d), and (f)) adsorption of PMo_{12} showing the molecules in cluster form.

Relationship between the RTS and the power spectral density

Figure S2 shows the time-domain signals, histograms of the time-domain signals, and the frequency-domain signals of the CNT devices after ZnPP adsorption. We observed identical corner frequencies in the power spectral densities (PSDs) of the current noise, regardless of whether the devices exhibited two-state or three-state RTSs, as well as in the case without any observable RTS. As mentioned in the main text, we believe that the corner frequency does not depend on the number of adsorbed molecules.

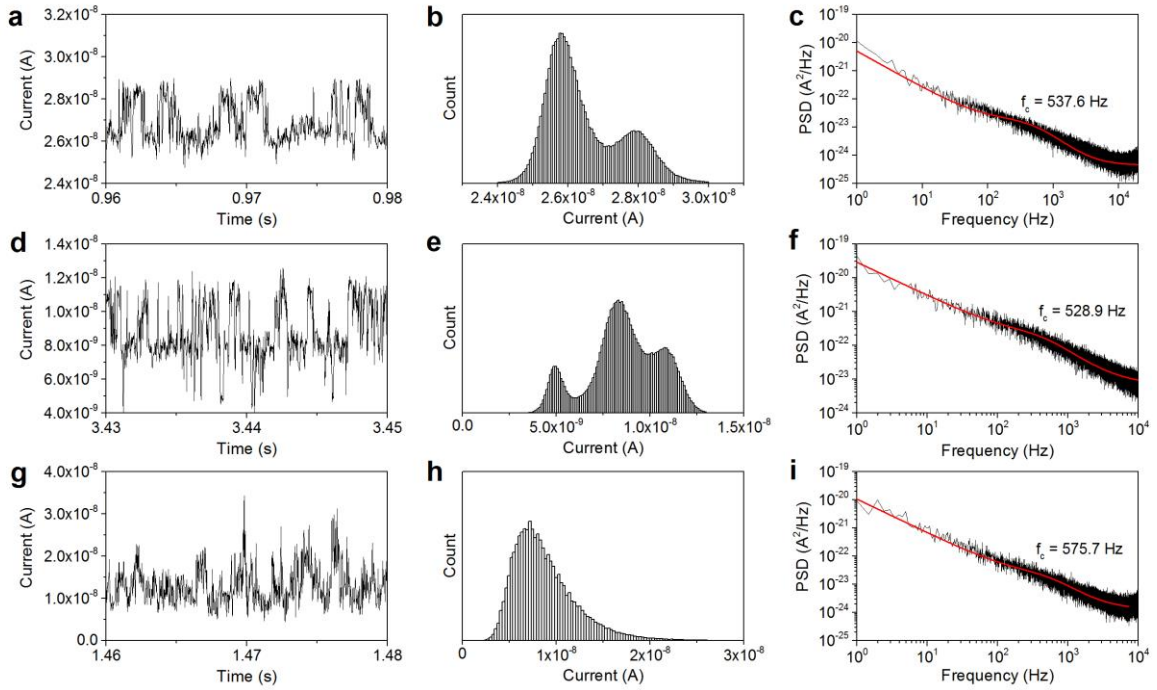

Figure S2. Identical PSD corner frequencies after ZnPP adsorption. (a), (b), and (c) show the time-domain signals, histograms of the time-domain signals, and the frequency-domain signals, respectively, from device-1, which exhibited two-state RTSs. (d), (e), and (f) show the time-domain signals, histograms of the time-domain signals, and frequency-domain signals, respectively, from device-2, having three-state RTSs. (g), (h), and (i) are the time-domain signals, histograms of the time-domain signals, and the frequency-domain signals, respectively, from device-3, without any observable RTS.

We also performed numerical simulations to demonstrate the effect of the number of molecules that provide RTS to the PSD of the current noise. We created the RTS by generating random numbers having a uniform distribution at a given time scale. We set the random duration of each pulse of these RTSs by generating a random number having an exponential distribution. We repeated the above steps 100 times and summed all of the RTS data to simulate the RTS from 100 molecules. The PSDs were obtained by fast Fourier transform followed by the application of a Gaussian filter. The PSDs were fitted using only the second term of Eq. 1 in the main text, S(f) = B/[1+(f/fc)2]. Figure S3 shows the results of our simulation. It is clear that the summation of 100 RTSs may obscure, but does not completely hide, the corner frequency of the Lorentzian-shaped PSD.

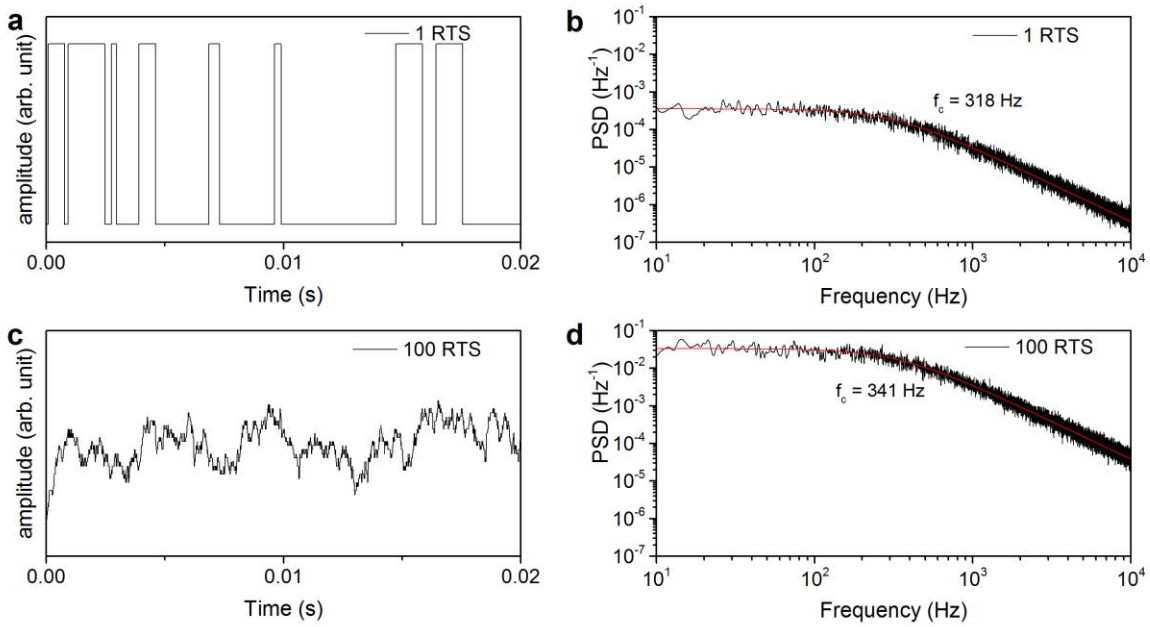

Figure S3. Numerical simulation of the RTS. (a) and (c) show the simulated RTS from 1 and 100 molecules, respectively. (b) and (d) show the power spectral density of the simulated RTS from 1 and 100 molecules, respectively.

Fitting of the RTS and its lifetime distribution

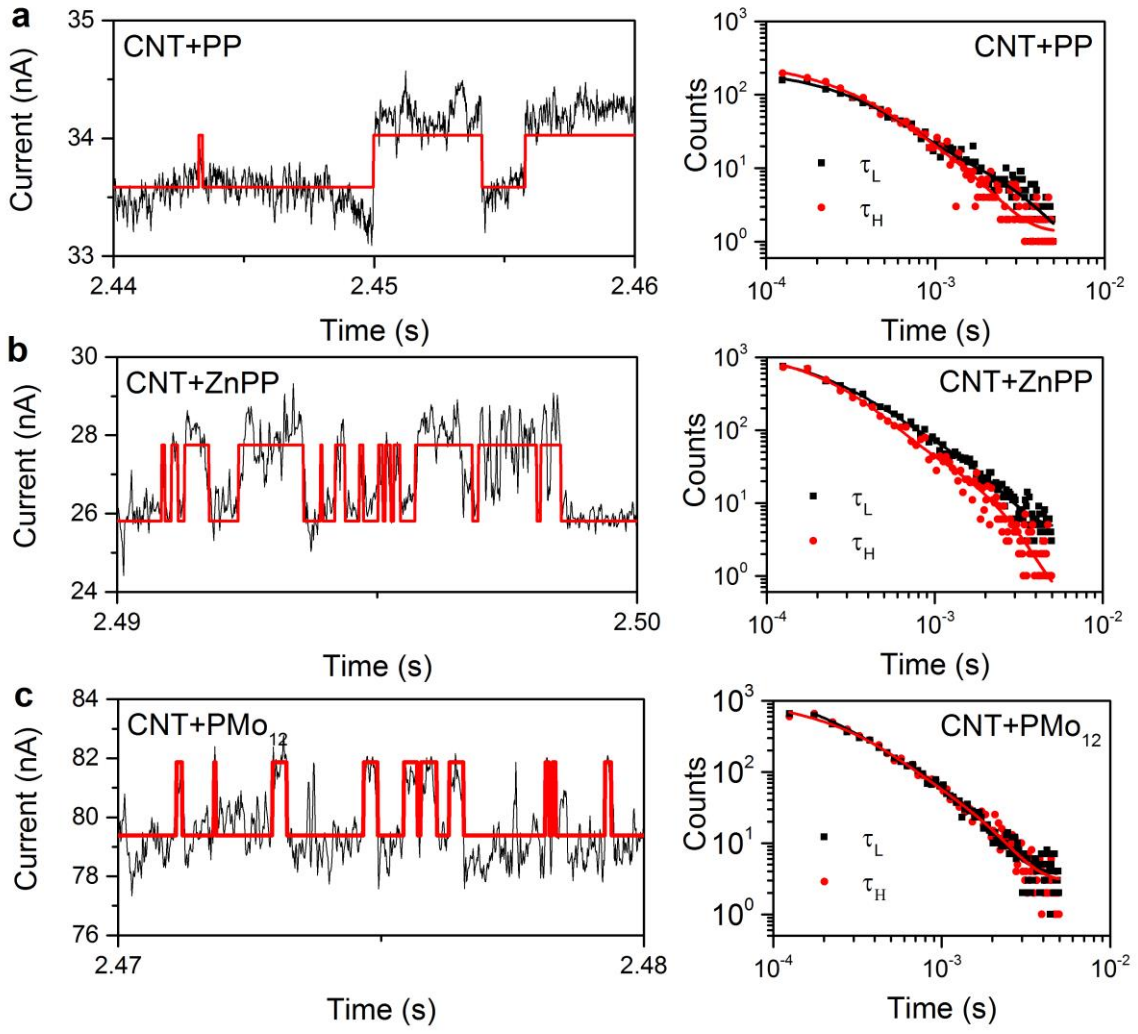

Figure S4. Fitting of the time-domain signal with the RTS using the hidden Markov model for the case of (a) CNT+PP, (b) CNT+ZnPP, and (c) CNT+PMo_{12}. The right-hand panel in each row show the lifetime distribution of the RTS signal, which was fitted using an exponential equation.

Temperature dependence of the RTS

Time-domain signals from room temperature to 200 K are shown in Fig. S5 for the case of PMo_{12}. The RTS lifetime increases as the temperature decreases, and the RTS begins to vanish at 200 K.

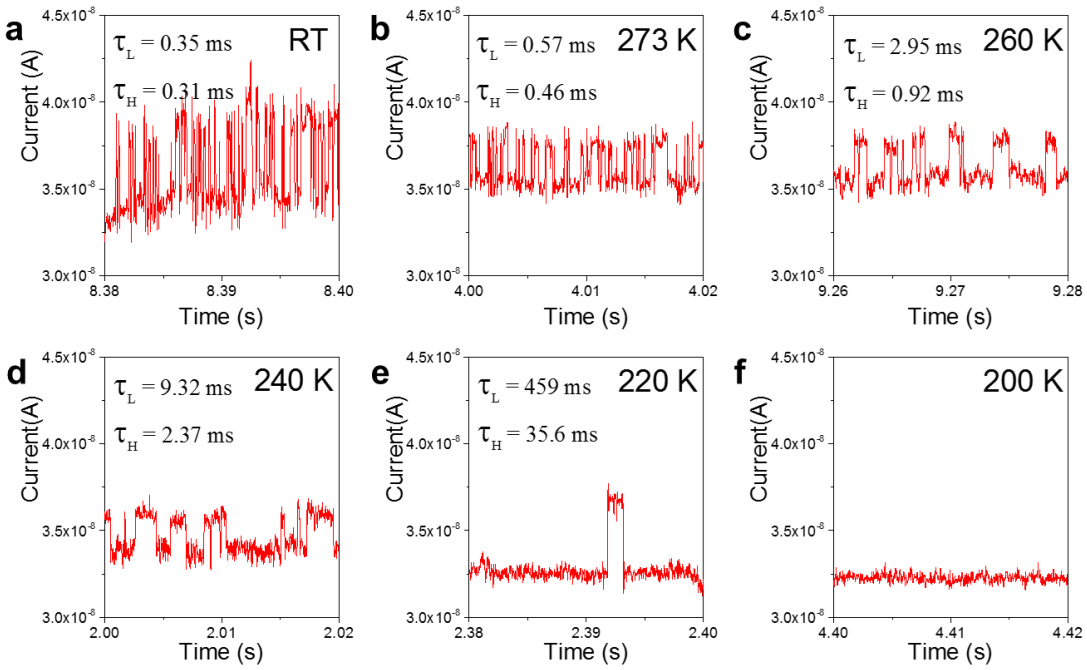

Figure S5. Temperature dependence of the RTS for CNT+PMo_{12}. (a), (b), (c), (d), (e), and (f) show the time-domain signals of the device at room temperature and at 273, 260, 240, 220, and 200 K, respectively, and $\bar{\tau}_L$ and $\bar{\tau}_H$ are the average RTS lifetimes. The RTS completely vanishes at 200 K.

Temperature dependence of the RTS

Figure S6 shows the cyclic voltammetry (CV) and differential pulse voltammetry (DPV) measurement results.

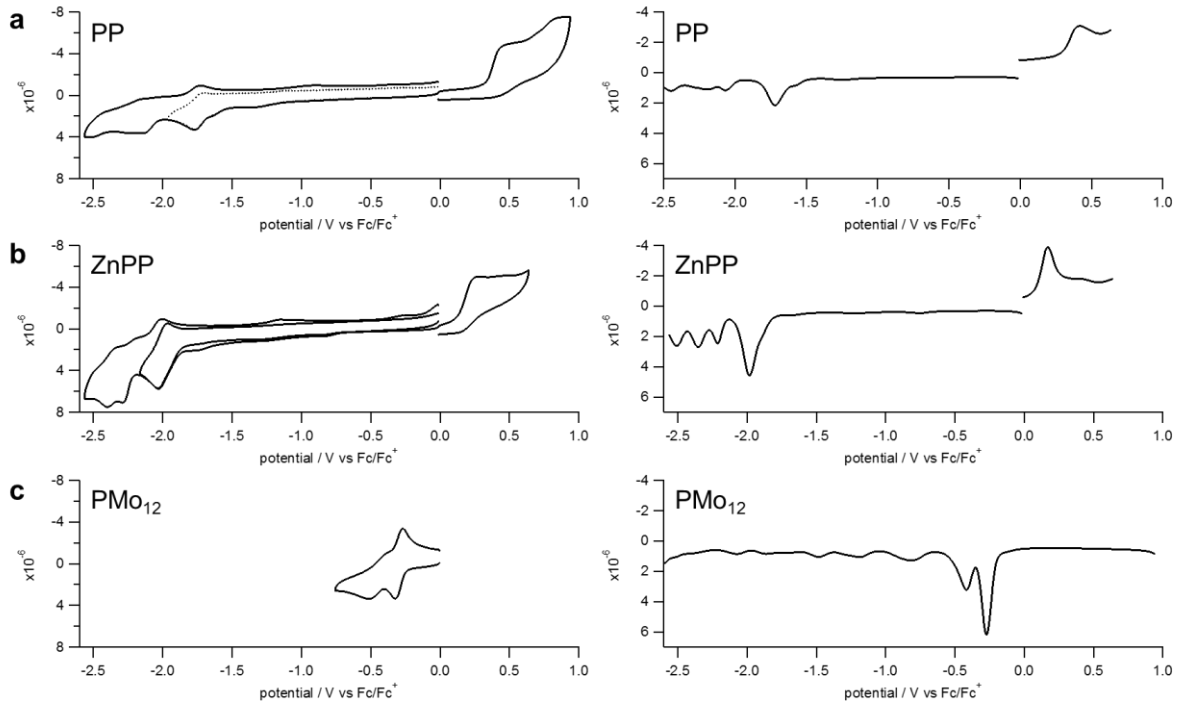

Figure S6. Results of electrochemical measurements. (a), (b), and (c) show the voltammetry measurement results for PP, ZnPP, and PMo_{12} molecules, respectively. The left- and right-hand panels show the CV and DPV curves, respectively.